Atg16L1 T300A variant decreases selective autophagy resulting in altered cytokine signaling and decreased antibacterial defense

Kara G. Lassen[a,b,1], Petric Kuballa[a,b,1], Kara L. Conway[a,b,c,1], Khushbu K. Patel[d], Christine E. Becker[b], Joanna M. Peloquin[b,c], Eduardo J. Villablanca[a,b,c], Jason M. Norman[d], Ta-Chiang Liu[d], Robert J. Heath[a,b], Morgan L. Becker[d], Lola Fagbami[a], Heiko Horn[a,e], Johnathan Mercer[a], Omer H. Yilmaz[f,g], Jacob D. Jaffe[a], Alykhan F. Shamji[h], Atul K. Bhan[g,i], Steven A. Carr[a], Mark J. Daly[a,i,j], Herbert W. Virgin[d,k], Stuart L. Schreiber[h,l,2], Thaddeus S. Stappenbeck[d], and Ramnik J. Xavier[a,b,c,i,2]

[a]Broad Institute, Cambridge, MA 02142; [b]Center for Computational and Integrative Biology, Massachusetts General Hospital, Boston, MA 02114; [c]Gastrointestinal Unit, Massachusetts General Hospital, Harvard Medical School, Boston, MA 02114; [d]Department of Pathology and Immunology, Washington University School of Medicine, St. Louis, MO 63110; [e]Department of Surgery, Massachusetts General Hospital, Harvard Medical School, Boston, MA 02114; [f]Koch Institute for Integrative Cancer Research and Department of Biology, Massachusetts Institute of Technology, Cambridge, MA 02139; [g]Pathology Department, Massachusetts General Hospital, Harvard Medical School, Boston, MA 02114; [h]Center for the Science of Therapeutics, Broad Institute, Cambridge, MA 02142; [i]Center for the Study of Inflammatory Bowel Disease, Massachusetts General Hospital, Boston, MA 02114; [j]Analytic and Translational Genetics Unit, Massachusetts General Hospital, Boston, MA 02114; [k]Department of Molecular Microbiology, Washington University School of Medicine, St. Louis, MO 63110; and [l]Department of Chemistry and Chemical Biology, Harvard University, Cambridge, MA 02138

Contributed by Stuart L. Schreiber, April 18, 2014 (sent for review March 10, 2014)

A coding polymorphism (Thr300Ala) in the essential autophagy gene, autophagy related 16-like 1 (*ATG16L1*), confers increased risk for the development of Crohn disease, although the mechanisms by which single disease-associated polymorphisms contribute to pathogenesis have been difficult to dissect given that environmental factors likely influence disease initiation in these patients. Here we introduce a knock-in mouse model expressing the Atg16L1 T300A variant. Consistent with the human polymorphism, T300A knock-in mice do not develop spontaneous intestinal inflammation, but exhibit morphological defects in Paneth and goblet cells. Selective autophagy is reduced in multiple cell types from T300A knock-in mice compared with WT mice. The T300A polymorphism significantly increases caspase 3- and caspase 7-mediated cleavage of Atg16L1, resulting in lower levels of full-length Atg16Ll T300A protein. Moreover, Atg16L1 T300A is associated with decreased antibacterial autophagy and increased IL-1β production in primary cells and in vivo. Quantitative proteomics for protein interactors of ATG16L1 identified previously unknown nonoverlapping sets of proteins involved in ATG16L1-dependent antibacterial autophagy or IL-1β production. These findings demonstrate how the T300A polymorphism leads to cell type- and pathway-specific disruptions of selective autophagy and suggest a mechanism by which this polymorphism contributes to disease.

Human genetic studies offer an unbiased approach to identify genes and DNA variants underlying susceptibility to complex diseases. Although this approach has been successful at identifying more than 160 loci associated with Crohn disease (CD), a chronic inflammatory condition affecting the gastrointestinal tract (1, 2), ascribing function to specific risk variants has been difficult. Individuals who harbor a common threonine to alanine coding variant at position 300 in autophagy related 16-like 1 (ATG16L1) (T300A) are at increased risk of developing CD compared with individuals who possess a threonine at this position (T300T) (3, 4). The T300A variant lies within a structurally unclassified region of ATG16L1, making it challenging to identify the effect of this polymorphism.

ATG16L1 is a component of the core autophagy machinery that plays a critical role in immunity and inflammation. Initial studies investigating ATG16L1 used hypomorphic Atg16L1 mouse models, which show Paneth cell abnormalities relevant to CD such as abnormal mitochondria, irregular patterns of granule morphology and lysozyme distribution, and increased expression of genes implicated in inflammation (5, 6). Although these studies have been useful in highlighting the important role of autophagy proteins in intestinal cells such as Paneth cells and goblet cells, the precise mechanisms by which ATG16L1 T300A influences pathogenesis remain unclear (7–10).

Previous studies have demonstrated that *Atg16L1*-deficient macrophages produce elevated levels of active caspase 1 and secrete higher levels of the cytokines IL-1β and IL-18 upon stimulation with the endotoxin LPS (5). Consistent with these results, peripheral blood mononuclear cells from patients homozygous for *ATG16L1* T300A produce increased levels of IL-1β upon muramyl dipeptide (MDP) stimulation compared with cells expressing T300T (11). Given the diverse roles of ATG16L1 and the canonical autophagy machinery in various cell types, investigating the effects of the T300A polymorphism on intestinal epithelial cells and gut-resident immune cells is critical to understanding the role of this polymorphism in CD pathogenesis.

Significance

Although advances in human genetics have shaped our understanding of many complex diseases, little is known about the mechanism of action of alleles that influence disease. By using mice expressing a Crohn disease (CD)-associated risk polymorphism (Atg16L1 T300A), we show that Atg16L1 T300A-expressing mice demonstrate abnormalities in Paneth cells (similar to patients with the risk polymorphism) and goblet cells. We show that Atg16L1 T300A protein is more susceptible to caspase-mediated cleavage than WT autophagy related 16-like 1 (Atg16L1), resulting in decreased protein stability and effects on antibacterial autophagy and inflammatory cytokine production. We also identify interacting proteins that contribute to autophagy-dependent immune responses. Understanding how ATG16L1 T300A modulates autophagy-dependent immune responses sheds light on the mechanisms that underlie initiation and progression of CD.

Author contributions: K.G.L., P.K., K.L.C., K.K.P., C.E.B., J.M.P., O.H.Y., T.S.S., and R.J.X. designed research; K.G.L., P.K., K.L.C., K.K.P., C.E.B., J.M.P., E.J.V., J.M.N., T.-C.L., R.J.H., M.L.B., L.F., and O.H.Y. performed research; K.G.L., P.K., K.L.C., K.K.P., C.E.B., J.M.P., E.J.V., J.M.N., T.-C.L., R.J.H., M.L.B., L.F., H.H., J.M., O.H.Y., J.D.J., A.F.S., A.K.B., S.A.C., M.J.D., H.W.V., S.L.S., T.S.S., and R.J.X. analyzed data; and K.G.L., K.L.C., and R.J.X. wrote the paper.

The authors declare no conflict of interest.

Freely available online through the PNAS open access option.

[1]K.G.L., P.K., and K.L.C. contributed equally to this work.

[2]To whom correspondence may be addressed. E-mail: stuart_schreiber@harvard.edu or xavier@molbio.mgh.harvard.edu.

This article contains supporting information online at www.pnas.org/lookup/suppl/doi:10.1073/pnas.1407001111/-/DCSupplemental.

A number of CD-associated genes, including *ATG16L1*, *NOD2* (nucleotide-binding oligomerization domain containing 2), and *IRGM*, have been associated with impaired intracellular bacterial handling. Previous studies have revealed that the ATG16L1–NOD2 axis is important for maintaining intracellular mucosal homeostasis and that the T300A polymorphism specifically disrupts antibacterial autophagy (12–14). Other studies have reported no association between the T300A polymorphism and antibacterial autophagy in reconstituted *Atg16L1*-deficient mouse embryonic fibroblasts (MEFs), suggesting that the T300A polymorphism confers cell type-specific effects (15).

Here we generated Atg16L1 T300A knock-in mice to examine the effects of the T300A polymorphism on various autophagy-dependent pathways. We show that Atg16L1 T300A is associated with impaired activation of autophagy against intracellular bacteria and increased IL-1β secretion. We identify and analyze previously unidentified ATG16L1 proteomic interactors to reveal ATG16L1-dependent, pathway-specific interactions.

Results

Atg16L1 T300A Mice Exhibit Defects in Paneth Cells and Goblet Cells. To investigate the in vivo effect of the ATG16L1 T300A polymorphism, we generated knock-in mice expressing Atg16L1 T300A (Fig. 1 *A* and *B* and Fig. S1 *A* and *B*). The position of the Thr-to-Ala substitution in murine Atg16L1 varies depending on the splice isoform expressed: T300A (isoform β), T281A (isoform α), or T316A (isoform γ) (16). Murine isoform β is the equivalent of human isoform 1, so these mice are hereafter referred to as T300A mice. T300A mice are viable, born at Mendelian ratios, and healthy, consistent with the high prevalence of the ATG16L1 polymorphism in healthy humans (3). Analysis of distal small intestine sections from WT and T300A mice housed in a specific pathogen-free facility revealed abnormal Paneth cell lysozyme distribution in T300A mice (Fig. 1 *C* and *D* and Fig. S1*C*),

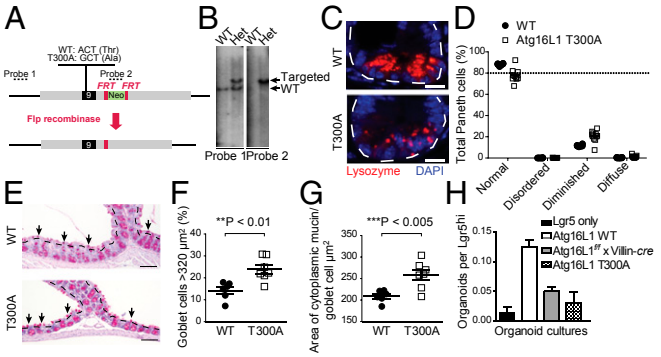

Fig. 1. Generation and characterization of T300A mice. (*A*) Schematic of targeted genomic region (gray), exon 9 (black), neomycin resistance cassette (green), and amino acids at position 300. Southern blot probes are indicated (dashed lines). (*B*) Genomic DNA of ES cells were detected via Southern blot. (*C*) Ileal sections were stained with lysozyme (red) and DAPI (blue). White dotted lines outline a single crypt. (Scale bar, 10 μm.) (*D*) Paneth cell phenotypes were classified as normal or abnormal (with disordered, diminished, diffuse, or excluded granule phenotypes) based on lysozyme-positive secretory granule morphology. Details of these categories are provided in *SI Materials and Methods*. (*E*) PAS/Alcian blue-stained colonic sections. Black dotted lines outline surface epithelium. Arrows indicate surface goblet cells. (Scale bar, 100 μm.) (*F*) Percentage of surface goblet cells (black arrows in *E*) greater than 320 μm^2. Data shown as mean ± SEM; n = 6–7 mice per group, n = 200–300 goblet cells per mouse (**$P < 0.01$). (*G*) Quantification of average goblet cell size (average area of cytoplasmic mucin/goblet cell) in WT and T300A ascending colon (n = 6 mice per group; ***$P < 0.005$, Student t test). (*H*) Organoid formation per WT Lgr5$^+$ intestinal stem cells cocultured with sorted Paneth cells from indicated mice (data shown as mean ± SD; $n \geq 4$).

similar to findings from patients with CD with T300A mutations (7, 17). Furthermore, analysis of Periodic acid–Schiff (PAS)-stained sections of murine colons revealed goblet cell abnormalities without alterations in goblet cell differentiation, similar to what was observed in mice with complete absence of autophagy proteins in the epithelium (Fig. 1 *E*–*G* and Fig. S1 *D* and *E*) (10). Here we observed enlarged goblet cells within the surface epithelial cuffs (but not within crypts) in T300A mice. This result is in contrast to mice with complete absence of autophagy proteins in the epithelium, which displayed enlarged goblet cells throughout the crypt–cuff axis (10). Abnormalities in goblet cell morphology were restricted to the colonic epithelium and were absent in the small intestinal epithelium (Fig. S1*F*). Thus, the T300A knock-in model recapitulates known CD Paneth cell phenotypes and uncovers a role for this polymorphism in the goblet cell compartment.

As a functional test for additional Paneth cell abnormalities, we performed an ex vivo organoid forming assay (18). Lgr5$^+$ stem cells were isolated from crypts of reporter mice and cultured alone or cocultured with Paneth cells isolated from WT mice, Atg16L1 T300A mice, or mice with *Atg16L1* deleted in the intestinal epithelium (Atg16L1$^{f/f}$ × Villin-*cre*) (19). Consistent with previous reports, coculture of Lgr5$^+$ stem cells with sorted Paneth cells from WT mice resulted in enhanced organoid formation (18) (Fig. 1*H*). However, coculture of Lgr5$^+$ epithelial cells with Paneth cells from Atg16L1 T300A mice or Atg16L1$^{f/f}$ × Villin-*cre* mice produced two- to threefold fewer organoids. Taken together, these results suggest that Paneth cells from Atg16L1 T300A mice are functionally defective in organoid formation, similar to Paneth cells that are autophagy-deficient, although the in vivo relevance of these findings remains to be determined (20).

Caspase 3 and Caspase 7 Preferentially Reduce ATG16L1 T300A Stability Compared with WT ATG16L1, Resulting in Altered Selective Autophagy. Given the essential role of ATG16L1 in autophagy, we next investigated whether the T300A polymorphism alters canonical or "bulk" autophagy. To test this hypothesis, we used immunoblots to assess the conversion of LC3-I to LC3-II via conjugation to phosphatidyl ethanolamine in MEFs from WT, Atg16L1 T300A, or Atg16Ll KO mice. At steady state, as well as in the presence of the lysosomal protease inhibitors E64d and pepstatin A, or in the presence of the mTORC1/2 inhibitor Torin 1 with E64d/pepstatin A, Atg16L1 T300A MEFs exhibited a small but consistent decrease in levels of LC3-II compared with WT MEFs, as well as an increase in levels of the autophagy substrate p62 (Fig. 2*A*). No changes were observed in levels of beclin 1 under these conditions (Fig. S2*A*). Under similar experimental conditions, cultures of primary intestinal epithelial cells also displayed decreased levels of LC3-II relative to controls (Fig. S2*B*). These results suggest modest effects of the T300A polymorphism in basal autophagy and in response to inducers of autophagy.

Previous data from our laboratory demonstrated that ATG16L1 T300A shows reduced protein stability upon infection with *Salmonella enterica* serovar Typhimurium (12). Examination of the amino acid sequence flanking T300A revealed that the polymorphism is directly preceded by the sequence DNVD, resembling the consensus motif DXXD for caspases 3 and 7 (Fig. 2*B*). Previous biochemical studies demonstrated that the amino acid immediately C-terminal to a caspase consensus motif influences the cleavage rate of a given substrate (21). These observations led us to hypothesize that the T300A polymorphism may alter the efficiency of caspase 3/7-mediated cleavage of ATG16L1.

To determine whether ATG16L1 is a substrate for caspases, we first performed in vitro caspase cleavage assays. ATG16L1 WT and T300A variants were in vitro translated with [^{35}S]methionine, and ^{35}S-labeled proteins were then incubated with human recombinant caspases. The T300A risk variant underwent almost complete fragmentation, whereas the WT variant was only partially cleaved by caspase 3 (Fig. 2 *C* and *D*). Caspase 7-mediated

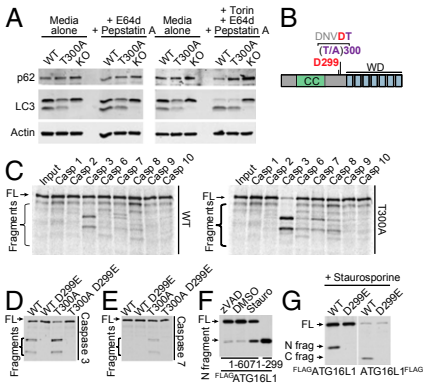

Fig. 2. ATG16L1 T300A is more susceptible to caspase 3- and caspase 7-mediated cleavage. (*A*) Immunoblot analysis of LC3-I/II and p62 in MEFs untreated or stimulated for 4 h with 10 μg/mL E64d plus pepstatin or 100 nM Torin 1 and 10 μg/mL E64d plus pepstatin. Blots were probed for LC3-I/II and p62. Actin served as a loading control. (*B*) Schematic of ATG16L1 domains with caspase cleavage consensus sequence and location of the T300A polymorphism. CC, coiled-coil domain. WD, WD40 domain. (*C*–*E*) ATG16L1 WT (isoform 1) or ATG16L1 T300A, with or without an additional D299E mutation, was in vitro-translated with [^{35}S]methionine and incubated with recombinant caspases for 1 h at 37 °C. ATG16L1 cleavage was observed by autoradiography. (*F* and *G*) Western blots showing ATG16L1 cleavage from HeLa cells transfected with indicated constructs and treated for 4 h with 1 μM staurosporine or 20 μM zVAD. FL, full-length.

cleavage of ATG16L1 T300A was also evident, particularly at higher concentrations of caspase 7 (Fig. 2 *C* and *E* and Fig. S2*C*). Caspases 6 and 8 did not generate ATG16L1 fragments even at high concentrations (Fig. 2*C* and Fig. S2*C*). These data suggest that ATG16L1 T300A is more susceptible to caspase 3- and caspase 7-mediated cleavage compared with the WT protein.

To confirm that these observations reflected caspase-mediated cleavage, we generated ATG16L1 expression constructs bearing a mutation in the caspase recognition site (ATG16L1 D299E), rendering this site inaccessible for caspases. ATG16L1 D299E was insensitive to cleavage by caspase 3 and 7 (Fig. 2 *D* and *E*). To further confirm caspase-mediated cleavage of ATG16L1, we transiently overexpressed ATG16L1 WT with a 3×FLAG tag at its N terminus (^{FLAG}ATG16L1) or C terminus (ATG16L1^{FLAG}) in HeLa cells. A cleavage product was readily detectable, which was diminished upon caspase inhibition (zVAD) and increased upon caspase activation (staurosporine), although ATG16L1 expression levels were lower with the C-terminal tag (Fig. 2 *F* and *G*). Increased caspase 3-mediated cleavage of ATG16L1 could also be observed in MEFs reconstituted with human ATG16L1 WT, T300A, and T300A-D299E variants (Fig. S2*D*). These data demonstrate the ATG16L1 is a target of caspase 3 and caspase 7 and that the T300A risk variant is more susceptible to this cleavage than the nonrisk variant. Consistent with these data, addition of a caspase 3 inhibitor or a caspase 3/7 inhibitor rescued autophagic flux in T300A MEFs (Fig. S2*E*).

Atg16L1 T300A Is Associated with Reduced Antibacterial Autophagy and Increased IL-1β Secretion in Vitro and in Vivo. Previous studies have shown that deletion of *Atg16L1* amplifies IL-1β signal transduction cascades (5). Significant increases in IL-1β production were observed in Atg16L1 T300A mesenteric lymph node dendritic cells, splenic CD11b$^+$ cells, and lamina propria CD11b$^+$ cells compared with WT cells (Fig. 3 *A* and *B*). This increase in IL-1β secretion was not associated with increased levels of pro–IL-1β (Fig. 3*A*). Of note, CD11b$^+$ cells isolated from the lamina propria, the site of CD, exhibited higher overall levels of IL-1β release, suggesting that these cells are a potent source of IL-1β (Fig. 3*B*). Moreover, secretion of IL-1β was enhanced when only one copy of the *Atg16L1* allele was present (Atg16L1 KO/WT) and increased further in the presence of the Atg16L1 T300A polymorphism (Atg16L1 KO/T300A; Fig. 3*C*), highlighting a direct role for Atg16L1 in IL-1β pathway regulation. Consistent results were also obtained when splenic macrophages were directly infected with *Shigella flexneri*, the etiologic agent of bacillary dysentery (Fig. 3*D*). No changes were observed in cell viability under these conditions (Fig. S3*A*). These data show that the Atg16L1 T300A polymorphism is sufficient to confer an increase in IL-1β secretion from multiple gut-resident inflammatory cell types.

Given the well-characterized role of ATG16L1 in antibacterial autophagy, we next determined whether the T300A polymorphism

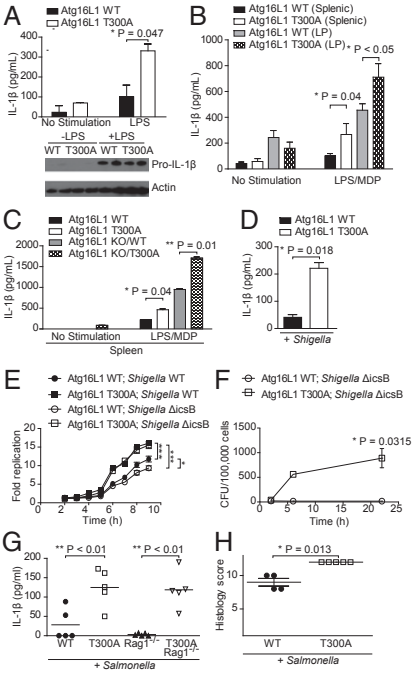

Fig. 3. T300A polymorphism enhances IL-1β secretion and is associated with increased susceptibility to bacteria-induced inflammation. (*A*) CD11c$^+$ cells were isolated from the mesenteric lymph node and stimulated with LPS. IL-1β levels in culture supernatants were assessed after 24 h (data shown as mean ± SD; $n = 2$; $^*P = 0.047$). Cell lysates were analyzed by Western blot for pro–IL-1β levels. Actin served as a loading control. (*B*) CD11b$^+$ cells were isolated from the spleen and colonic lamina propria (LP) and stimulated with LPS and MDP. IL-1β levels in culture supernatants were assessed after 24 h (data shown as mean ± SD; $n \geq 5$; $^*P = 0.04$, WT vs. T300A splenic; $^*P < 0.05$, WT vs. T300A lamina propria). (*C*) CD11b$^+$ cells were isolated from the spleen and stimulated with LPS and MDP. IL-1β levels in culture supernatants were assessed after 24 h (data shown as mean ± SD; $n = 10$; $^*P = 0.04$, WT vs. T300A; $^{**}P = 0.01$, ATG16L1 KO/WT vs. ATG16L1 KO/T300A). (*D*) CD11b$^+$ cells were isolated from the spleen and infected with *S. flexneri*. IL-1β levels in culture supernatants were assessed after 16 h. (Data shown as mean ± SD and are representative of $n = 3$; $^*P = 0.018$). (*E*) *S. flexneri* or *S. flexneri* ΔicsB survival as assessed by an intracellular bacterial protection assay. Relative bacterial luciferase units were measured in live MEFs at the indicated times postinfection. Fold replication was calculated for each well as raw luciferase units at the indicated time point divided by raw luciferase units at t 1.5 h ($n = 4$; data shown as mean ± SD; $^{***}P < 0.0004$, Atg16L1 WT vs. T300A with *Shigella* WT; $^{***}P < 10^{-5}$, Atg16L1 WT vs. T300A with *Shigella* ΔicsB; $^*P = 0.02$, *Shigella* WT vs. *Shigella* ΔicsB in Atg16L1 WT MEFs). (*F*) *S. flexneri* ΔicsB intracellular replication in small intestinal epithelial cells. Fold replication was calculated for each well as cfu counts per 100,000 cells at the indicated time point/raw luciferase units ($n > 3$; $^*P = 0.0315$). (*G*) Serum IL-1β levels 6 d after *S.* Typhimurium infection ($n \geq 4$; $^{**}P < 0.01$, WT vs. T300A; $^{**}P < 0.01$, Rag1 KO vs. T300A Rag1 KO). (*H*) Histological score for inflammation in cecal tissues 6 d after *S.* Typhimurium infection (data shown as mean ± SD; $n \geq 4$; $^*P = 0.013$).

alters antibacterial autophagy by performing an intracellular replication assay by using *Shigella*. *Shigella* was used as a model pathogen because it is known to partially escape autophagy through the production of the bacterial protein IcsB and is associated with IL-1β production (22). WT *Shigella* exhibited increased replication in Atg16L1 T300A MEFs compared with WT MEFs (Fig. 3*E*). This difference was further enhanced when the *Shigella* ΔicsB mutant was used, suggesting that the increase in intracellular replication was a result of impaired antibacterial autophagy in Atg16L1 T300A MEFs (Fig. 3*E* and Fig. S3*B*). *Shigella* infection of primary cultures also resulted in decreased epithelial integrity (Fig. S3*C*) as well as increased intracellular bacterial replication (Fig. 3*F*) in Atg16L1 T300A cells compared with WT cells. Decreased epithelial integrity was similar in Atg16L1 T300A and the autophagy-deficient Atg16L1$^{f/f}$ × Villin-*cre* cells after infection. These findings are consistent with defects in selective autophagy in Atg16L1 T300A, as differences are observed only in the presence of bacterial infection.

Our group as well as others recently demonstrated that Atg16L1 regulates autophagy in intestinal epithelial cells and is required for bacterial clearance of *S.* Typhimurium in vivo (9, 20). To assess whether the Atg16L1 T300A polymorphism impairs antibacterial autophagy and immune responses in vivo, we next infected T300A mice with *S.* Typhimurium. This model induces acute inflammation in the cecum and colon and depends largely on the coordinated responses of the epithelial cell and macrophage compartments. Having demonstrated hypersecretion of IL-1β from Atg16L1 T300A primary dendritic cells and CD11b^{+} cells, we assessed serum IL-1β levels 6 d after *S*. Typhimurium infection. Systemic IL-1β was detected in all mice, but was significantly higher in Atg16L1 T300A knock-in mice (Fig. 3*G*). The T300A-induced increased IL-1β secretion originated largely from nonlymphocyte compartments, as T300A × *Rag1*$^{-/-}$ mice showed IL-1β levels similar to T300A lymphocyte-replete mice (Fig. 3*G*), consistent with the phenotypes observed in the ex vivo cellular assays. In addition, Atg16L1 T300A mice developed more severe inflammation than WT mice 6 d after *S.* Typhimurium infection (Fig. 3*H* and Fig. S3*D*). Thus, expression of Atg16L1 T300A alters immune responses and compromises host defenses during pathogenic *S*. Typhimurium infection.

Quantitative Proteomics Identifies ATG16L1 Interactors Involved in Antibacterial Autophagy and IL-1β Secretion. To identify new protein interactors involved in ATG16L1-mediated IL-1β secretion and antibacterial autophagy, we next performed iTRAQ (isobaric tags for relative and absolute quantification) proteomics. To obtain high-confidence interactions, we expressed multiple FLAG-tagged human ATG16L1 isoforms (WT isoform 1, WT isoform 2, and T300A) in autophagy-deficient MEFs (Fig. 4*A*). Proteomic interactors were defined as those that showed significantly increased binding to any ATG16L1 isoform compared with the expression of empty vector alone. Our proteomic analysis identified a number of known ATG16L1 interactions, including Atg3, Atg5, Atg12, and Rab33b (23, 24). Additionally, we identified Gcat, Slc25a11 [solute carrier family 25 (mitochondrial carrier oxoglutarate carrier), member 11], Suclg1 (succinate-CoA ligase GDP-forming alpha subunit), and Vps28 (vacuolar protein sorting 28), which were previously shown to be part of the high-confidence autophagy interaction network (23). Of the 40 previously unidentified ATG16L1 protein interactions identified, we selected a subset for follow-up analysis (Fig. 4*B* and Dataset S1). An interactome-based affiliation scoring method was used to analyze the proteins identified by iTRAQ proteomics, and this interactome analysis resulted in a significant connected network (area under the receiver-operating characteristic, 0.59; $P = 0.01$) containing a subset of proteins associated with autophagosomal formation, as expected ($P < 8.83 \times 10^{-7}$; Fig. 4*C* and Fig. S4) (25).

To determine if any of these genes play a role in IL-1β secretion, we knocked down expression of individual genes by using lentiviral shRNA transduction in WT immortalized bone marrow-derived macrophages (BMDMs; Fig. S5*A*). shRNA-transduced BMDMs were stimulated with LPS and MDP overnight, and IL-1β secretion was measured by ELISA. Increased IL-1β secretion was consistently observed in cells transduced with shRNAs against *Suclg1*, *Mccc2*, *Slc25a11*, and *Vps28* (Fig. 4*D* and Fig. S5*B*). Knockdown at the RNA level was confirmed by quantitative PCR (qPCR; Fig. S5*C* and Table S1). None of the shRNAs significantly changed the levels of IL-1β mRNA in the absence of stimulation, suggesting the increase in IL-1β secretion was dependent on LPS and MDP (Fig. S5*D*).

We next evaluated the role of the selected interactors in antibacterial autophagy by using siRNA in HeLa cells. We chose to use *S.* Typhimurium as a model pathogen because of its well-characterized susceptibility to autophagy in HeLa cells (12, 26, 27). Of the tested genes, six [*BTD*, *AVIL*, *GARS*, *CALU*, *NOLC1* (nucleolar and coiled-body phosphoprotein 1), and *SLC25A11*] showed reproducible phenotypes in both LC3–*Salmonella* colocalization and intracellular bacterial replication assays, suggesting roles for these genes in antibacterial autophagy (Fig. 4 *E* and *F* and Fig. S5*E*). We selected *NOLC1* and *BTD* for further analysis. Decreased colocalization of LC3 and *Salmonella* in siNOLC1- and siBTD-treated cells was confirmed with confocal microscopy, and knockdown was confirmed by qPCR in infected and uninfected cells (Fig. 4*G*, Fig. S5 *F* and *G*, and Table S1). Knockdown of *NOLC1*, but not *BTD*, affected NDP52 colocalization, suggesting that *NOLC1* functions slightly upstream of ATG16L1 (Fig. 4 *H* and *I*). Taken together, our proteomic analysis identified sets of genes involved in ATG16L1-dependent IL-1β secretion and antibacterial autophagy.

Discussion

Our results support the growing recognition that autophagy genes and the pathways in which they participate are a common link between many of the identified genetic loci for CD and inflammatory bowel disease (IBD). Although no epistasis has been demonstrated between the >160 identified loci for IBD, it is clear that genetic epistasis exists at the level of autophagy, a pathway that lies at the intersection of cellular stress, metabolic regulation, and immunity. Notably, although genome-wide association studies and subsequent follow-up studies have revealed a strong link between autophagy genes and IBD, no such connection has been reported for celiac disease or other autoimmune diseases (1). High bacterial loads are present in the terminal ileum, the site of CD, suggesting a prominent physiologic role for autophagy (bulk or selective) in interactions with bacteria (9). This prospect points to a potential key role for antibacterial autophagy in CD pathogenesis, consistent with our findings that the presence of the Atg16L1 T300A variant in mice is associated with impaired antibacterial autophagy and increased production of the proinflammatory cytokine IL-1β. A recent study has also suggested decreased antibacterial autophagy of the ileal pathogen *Yersinia enterocolitica* in ATG16L1 T300A cells (28), demonstrating that reduced antibacterial autophagy in Atg16L1 T300A cells is not pathogen-specific and suggesting that various environmental microbial triggers can be associated with disease.

Together these data suggest a model in which Atg16L1 T300A reduces, but does not eliminate, selective autophagy. In this model, disrupted epithelial integrity associated with pathogenic bacterial infection in Atg16L1 T300A may result in increased cellular invasion of opportunistic commensal bacteria and subsequent increased cellular bacterial load. Furthermore, we demonstrated enhanced bacterial replication in epithelial cells expressing ATG16L1 T300A, as well as aberrant Paneth cell and goblet cell morphologies in Atg16L1 T300A mice, all suggestive

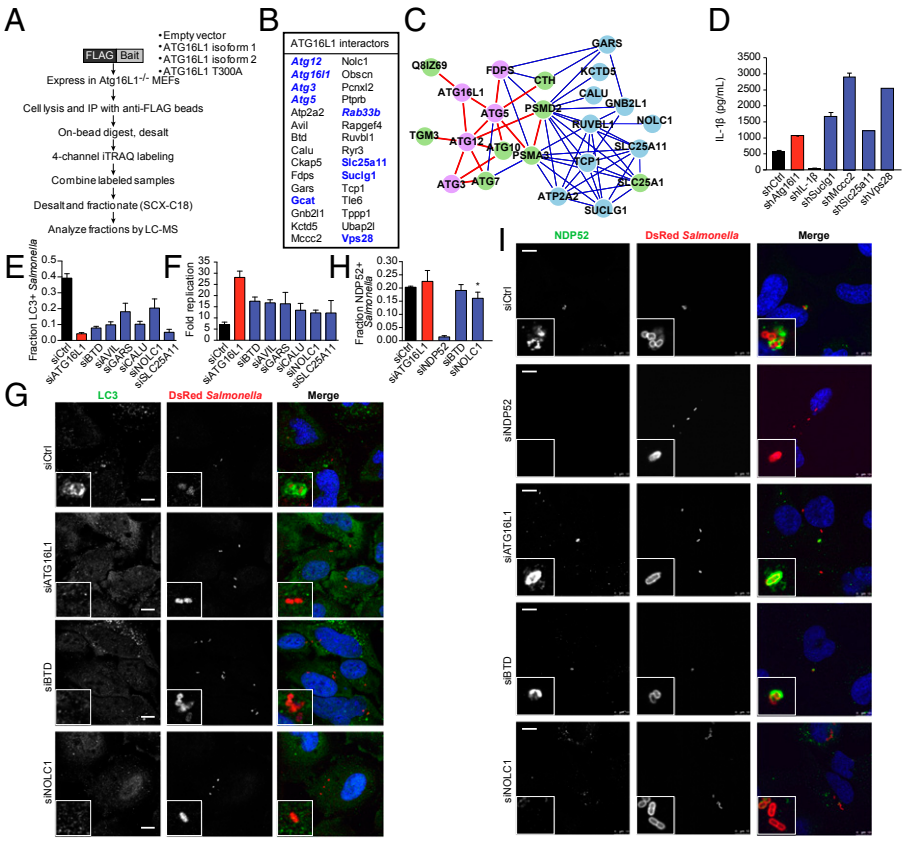

Fig. 4. Quantitative proteomics identifies ATG16L1-dependent proteins involved in IL-1β secretion and antibacterial autophagy. (*A*) Schematic of quantitative iTRAQ proteomic experimental design. Atg16L1$^{-/-}$ MEFs were transfected with empty vector, FLAG-WT hATG16L1 isoform 1, FLAG-hATG16L1 isoform 2, or FLAG-hATG16L1 T300A. Immunoprecipitated complexes were labeled, combined, and analyzed by liquid chromatography/MS. (*B*) Summary of proteomic interactors selected for follow-up analysis. Proteins in bold were previously identified as members of the autophagy interactome (23); proteins also in italics were previously identified as ATG16L1 interactors. (*C*) Interactome analysis shows network after extension. Proteins identified by proteomics are shown in purple and blue, with high-confidence autophagy-associated genes shown in purple. Intervening nodes are shown in green. High-confidence interactions are shown with red lines, and lower-confidence interactions are visualized with blue lines. (*D*) Immortalized BMDMs were infected with the indicated shRNA lentiviruses, and transduced cells were selected with puromycin. Cells were stimulated with IFN-γ (100 ng/mL), LPS (100 ng/mL), and MDP (10 μg/mL) for 24 h, and harvested supernatants were analyzed by ELISA for IL-1β secretion (data shown as mean ± SD; $n = 4$). (*E*) HeLa cells stably transduced with GFP-LC3 were transfected for 48 h with control siRNA or siRNAs against the indicated genes and then infected with DsRed-labeled *Salmonella* for 1 h. GFP-LC3/bacteria colocalization was measured at six sites per well, and data shown are mean ± SD of three wells per condition. Data are representative of three independent experiments. (*F*) *Salmonella* survival as assessed by an intracellular bacterial protection assay in HeLa cells treated with the indicated siRNA for 48 h. Fold replication was calculated for each well as raw luciferase units at the indicated time point divided by raw luciferase units at *t* 1.5 h (data shown as mean ± SD; $n = 3$). (*G*) Representative confocal fluorescence microscopy images of HeLa cells treated as described in *E*. (*H*) siRNA-treated cells were infected as described in *E* and stained with anti-NDP52. NDP52/bacteria colocalization was measured at six sites per well, and data shown are mean ± SD of three wells per condition. Data are representative of three independent experiments (*$P = 0.045$, siCtrl vs. siNOLC1). (*I*) Representative confocal fluorescence microscopy images of HeLa cells treated as in *G*.

of impaired bacterial defense mechanisms in the presence of the risk polymorphism. Consistent with these data, a recent report has suggested a link between autophagy, inflammasome activation, and mucus secretion in colonic goblet cells (29). Notably, we found that bacterial infection alone was sufficient to induce higher levels of IL-1β in Atg16L1 T300A inflammatory immune cells. These findings illustrate how small alterations in autophagy can have different consequences that phenotypically converge in pathogenesis. Viewed in the context of many recent studies reporting strong phenotypes associated with complete KO of autophagy genes in selected cell types (30), our results highlight specific processes and cell types, such as Paneth and goblet cells, that are particularly sensitive to the relatively subtle inhibition in this pathway that occurs with Atg16L1 T300A expression. We note that the Paneth cell phenotype described here is in contrast to a recent report (28); these differences may result from the increased sensitivity and resolution afforded by our staining techniques. It will also be important for future studies to investigate the molecular cross-talk between specific cell types expressing Atg16L1 T300A.

We found that the observed T300A-dependent phenotypes are associated with deficiencies in protein stability as a result of increased cleavage of ATG16L1 T300A by caspase 3 or caspase 7. Although caspase 3 more potently cleaves T300A compared with similar levels of caspase 7, in vivo cleavage of ATG16L1 is likely dependent on the relative expression of caspases 3 and 7 in different cell types. These results are consistent with recent reports evaluating the mechanism underlying the ATG16L1 T300A polymorphism (28). Caspase dysfunction has been previously associated with IBD and mucosal inflammation (31). Under conditions of cellular stress in which caspase activation is known to occur, ATG16L1 T300A-mediated autophagy is particularly impaired (28). Interestingly, a protective missense SNP in the gene encoding amyloid-β precursor protein (APP) has been shown to alter cleavage of full-length APP by aspartyl protease, suggesting that alterations of proteolytic cleavage could be a common feature of disease-associated SNPs

(32). Small molecule development to treat complex diseases may focus on disruption of SNP-dependent protease–substrate interactions, suggesting an important avenue for development of therapeutic agents in addition to compounds that can enhance autophagy.

In this study, we used functional genetics to place six ATG16L1-interacting genes in the antibacterial autophagy pathway and four ATG16L1-interacting genes in the IL-1β pathway. Interestingly, our assays did not demonstrate a high degree of overlap between ATG16L1-dependent genes involved in antibacterial autophagy and IL-1β secretion, suggesting that, outside of the core autophagy machinery, discrete sets of genes confer specificity to ATG16L1 function. Our results also demonstrate that ATG16L1 interactors function at discrete steps in antibacterial autophagy based on NDP52 colocalization. VPS28, a member of the endosomal sorting complex required for transport (ESCRT)-1 complex, was previously identified as a negative regulator of NOD2 signaling (33), suggesting that ATG16L1 interactors may be acting with cellular proteins at multiple steps in the IL-1β signaling cascade (11, 34). This finding illustrates how our studies have identified pathway-specific proteomic interactors that suggest therapeutic entry points to modulate specific arms of ATG16L1 function (9, 35).

Materials and Methods

Antibacterial Autophagy Assays. Antibacterial autophagy assays were performed as described previously (36, 37). Additional details are provided in *SI Materials and Methods*. For in vivo *Salmonella* infection, bacterial growth and infection were performed as previously described (9). Mice were killed via CO_2 asphyxiation 6 d after *S.* Typhimurium infection, at which point serum and tissues were harvested. Histology and pathology scoring are described in detail in *SI Materials and Methods*.

Analysis of IL-1β Secretion. IL-1β was detected by sandwich ELISA per manufacturer's protocol (BD Biosciences). Samples were quantified by using the SpectraMax M5 microplate reader (Molecular Devices), measuring absorbance at 450 nm. Protocols for immune cell isolation, stimulation, and shRNA infection are described in detail in *SI Materials and Methods*.

ACKNOWLEDGMENTS. We thank Natalia Nedelsky for editorial assistance and Brian Seed and Naifang Liu for help with the knock-in model design. This work was supported by the Leona M. and Harry B. Helmsley Charitable Trust, the Crohn's and Colitis Foundation of America Genetics Initiative, National Institutes of Health Grants DK097485 and DK043351 (to R.J.X.) and AI084887 (to T.S.S. and H.W.V.), and Deutsche Forschungsgemeinschaft Fellowship Award KU2511/1-1 (to P.K.).

1. Jostins L, et al.; International IBD Genetics Consortium (IIBDGC) (2012) Host-microbe interactions have shaped the genetic architecture of inflammatory bowel disease. *Nature* 491(7422):119–124.
2. Franke A, et al. (2010) Genome-wide meta-analysis increases to 71 the number of confirmed Crohn's disease susceptibility loci. *Nat Genet* 42(12):1118–1125.
3. Rioux JD, et al. (2007) Genome-wide association study identifies new susceptibility loci for Crohn disease and implicates autophagy in disease pathogenesis. *Nat Genet* 39(5): 596–604.
4. Khor B, Gardet A, Xavier RJ (2011) Genetics and pathogenesis of inflammatory bowel disease. *Nature* 474(7351):307–317.
5. Saitoh T, et al. (2008) Loss of the autophagy protein Atg16L1 enhances endotoxin-induced IL-1beta production. *Nature* 456(7219):264–268.
6. Cadwell K, et al. (2010) Virus-plus-susceptibility gene interaction determines Crohn's disease gene Atg16L1 phenotypes in intestine. *Cell* 141(7):1135–1145.
7. Cadwell K, et al. (2008) A key role for autophagy and the autophagy gene Atg16l1 in mouse and human intestinal Paneth cells. *Nature* 456(7219):259–263.
8. Adolph TE, et al. (2013) Paneth cells as a site of origin for intestinal inflammation. *Nature* 503(7475):272–276.
9. Conway KL, et al. (2013) Atg16l1 is required for autophagy in intestinal epithelial cells and protection of mice from Salmonella infection. *Gastroenterology* 145(6): 1347–1357.
10. Patel KK, et al. (2013) Autophagy proteins control goblet cell function by potentiating reactive oxygen species production. *EMBO J* 32(24):3130–3144.
11. Plantinga TS, et al. (2011) Crohn's disease-associated ATG16L1 polymorphism modulates pro-inflammatory cytokine responses selectively upon activation of NOD2. *Gut* 60(9):1229–1235.
12. Kuballa P, Huett A, Rioux JD, Daly MJ, Xavier RJ (2008) Impaired autophagy of an intracellular pathogen induced by a Crohn's disease associated ATG16L1 variant. *PLoS ONE* 3(10):e3391.
13. Travassos LH, et al. (2010) Nod1 and Nod2 direct autophagy by recruiting ATG16L1 to the plasma membrane at the site of bacterial entry. *Nat Immunol* 11(1):55–62.
14. Cooney R, et al. (2010) NOD2 stimulation induces autophagy in dendritic cells influencing bacterial handling and antigen presentation. *Nat Med* 16(1):90–97.
15. Fujita N, et al. (2009) Differential involvement of Atg16L1 in Crohn disease and canonical autophagy: Analysis of the organization of the Atg16L1 complex in fibroblasts. *J Biol Chem* 284(47):32602–32609.
16. Zheng H, et al. (2004) Cloning and analysis of human Apg16L. *DNA Seq* 15(4):303–305.
17. VanDussen KL, et al. (2014) Genetic variants synthesize to produce Paneth cell phenotypes that define subtypes of Crohn's disease. *Gastroenterology* 146(1):200–209.
18. Sato T, et al. (2011) Paneth cells constitute the niche for Lgr5 stem cells in intestinal crypts. *Nature* 469(7330):415–418.
19. Korn LL, et al. (2014) Conventional CD4+ T cells regulate IL-22-producing intestinal innate lymphoid cells. *Mucosal Immunol*, 10.1038/mi.2013.121.
20. Kim TH, Escudero S, Shivdasani RA (2012) Intact function of Lgr5 receptor-expressing intestinal stem cells in the absence of Paneth cells. *Proc Natl Acad Sci USA* 109(10): 3932–3937.
21. Mahrus S, et al. (2008) Global sequencing of proteolytic cleavage sites in apoptosis by specific labeling of protein N termini. *Cell* 134(5):866–876.
22. Ogawa M, et al. (2005) Escape of intracellular Shigella from autophagy. *Science* 307(5710):727–731.
23. Behrends C, Sowa ME, Gygi SP, Harper JW (2010) Network organization of the human autophagy system. *Nature* 466(7302):68–76.
24. Itoh T, et al. (2008) Golgi-resident small GTPase Rab33B interacts with Atg16L and modulates autophagosome formation. *Mol Biol Cell* 19(7):2916–2925.
25. Miraoui H, et al. (2013) Mutations in FGF17, IL17RD, DUSP6, SPRY4, and FLRT3 are identified in individuals with congenital hypogonadotropic hypogonadism. *Am J Hum Genet* 92(5):725–743.
26. Thurston TL, Wandel MP, von Muhlinen N, Foeglein A, Randow F (2012) Galectin 8 targets damaged vesicles for autophagy to defend cells against bacterial invasion. *Nature* 482(7385):414–418.
27. Orvedahl A, et al. (2011) Image-based genome-wide siRNA screen identifies selective autophagy factors. *Nature* 480(7375):113–117.
28. Murthy A, et al. (2014) A Crohn's disease variant in Atg16l1 enhances its degradation by caspase 3. *Nature* 506(7489):456–462.
29. Wlodarska M, et al. (2014) NLRP6 inflammasome orchestrates the colonic host-microbial interface by regulating goblet cell mucus secretion. *Cell* 156(5):1045–1059.
30. Patel KK, Stappenbeck TS (2013) Autophagy and intestinal homeostasis. *Annu Rev Physiol* 75:241–262.
31. Becker C, Watson AJ, Neurath MF (2013) Complex roles of caspases in the pathogenesis of inflammatory bowel disease. *Gastroenterology* 144(2):283–293.
32. Jonsson T, et al. (2012) A mutation in APP protects against Alzheimer's disease and age-related cognitive decline. *Nature* 488(7409):96–99.
33. Warner N, et al. (2013) A genome-wide siRNA screen reveals positive and negative regulators of the NOD2 and NF-κB signaling pathways. *Sci Signal* 6(258):rs3.
34. Harris J, et al. (2011) Autophagy controls IL-1beta secretion by targeting pro-IL-1beta for degradation. *J Biol Chem* 286(11):9587–9597.
35. Shaw SY, et al. (2013) Selective modulation of autophagy, innate immunity, and adaptive immunity by small molecules. *ACS Chem Biol* 8(12):2724–2733.
36. Huett A, et al. (2009) A novel hybrid yeast-human network analysis reveals an essential role for FNBP1L in antibacterial autophagy. *J Immunol* 182(8):4917–4930.
37. Huett A, et al. (2012) The LRR and RING domain protein LRSAM1 is an E3 ligase crucial for ubiquitin-dependent autophagy of intracellular Salmonella Typhimurium. *Cell Host Microbe* 12(6):778–790.